

## Electron spectra from multiphoton ionization of xenon at 1064, 532, and 355 nm

P. Kruit, J. Kimman, H. G. Muller, and M. J. van der Wiel

*FOM—Institute for Atomic and Molecular Physics (Fundamenteel Onderzoek der Materie—Instituut voor Atoom- en Molecuulfysica), Kruislaan 407, 1098 SJ Amsterdam, The Netherlands*

(Received 6 December 1982)

We report an electron spectroscopy study of continuum-continuum transitions that follow multiphoton ionization. Xenon was ionized by 10-ns multimode pulses at wavelengths of 1064, 532, and 355 nm, at intensities up to  $10^{13}$  W/cm<sup>2</sup>. The photoelectrons are confined by a diverging magnetic field and energy analyzed by means of the time-of-flight technique. Our setup allows an acceptance angle of  $2\pi$  sr at an energy resolution of 15 meV. At a wavelength of 1064 nm, 11-photon ionization is energetically allowed but we report spectra in which the 12- and up to 19-photon ionization processes show higher relative probabilities. The intensity dependence of the separate processes gives a result that deviates strongly from lowest-order perturbation theory. An interpretation of the width of the peaks in the electron spectra based on the ponderomotive force is proposed.

### I. INTRODUCTION

In the application of high-energy pulsed lasers quite often the heating of electrons plays an important role. Models of the heating process lack information on fundamental processes like free-free absorption and continuum-continuum transitions directly following multiphoton ionization.

Apart from the practical relevance, a study of the energy of electrons arising from multiphoton ionization can contribute to the theory of highly nonlinear processes. In this theory the present question is up to which limits the perturbation approach is adequate.

Until a few years ago the study of multiphoton ionization was restricted to the measurement of the intensity and wavelength dependence of the total ionization probability. Only recently electron spectrometers have been employed to study the effect of additional photon absorption, also called "continuum-continuum transitions" or "above threshold ionization."<sup>1-3</sup> From lowest-order perturbation theory the  $N$ -photon ionization probability is expected to increase with the  $N$ th power of the light intensity,  $N$  being the first integer for which  $N$  times the photon energy exceeds the ionization potential. The  $(N+1)$ -photon process, yielding an electron with more kinetic energy than the  $N$ -photon process, is expected to increase with the  $(N+1)$ th power of the light intensity, etc.<sup>4-6</sup> Simple extrapolation of the lowest-order perturbation theory leads to the conclusion that there should be an intensity regime in which the  $(N+1)$ -photon process is more probable than the  $N$ -photon process. However, the requirement for a perturbation method to be applicable is that  $(x+1)$ -order processes are less probable than  $x$ -order processes.

For experimental studies in this intensity regime with a Nd-YAG (yttrium aluminum garnet) laser (1064 nm), one is limited in the choice of the target atom. For example, in our experiments with a 10-ns pulse, the ionization of the theoretically attractive cesium atom is already saturated at intensities in which the probability of additional photon absorption is only 1%. Thus we had to choose an atom with higher ionization potential. We chose xenon, although xenon is more complicated, because the atom has

two ionization potentials (see Fig. 1): 12.127 eV for the  $^2P_{3/2}$  core and 13.44 eV for the  $^2P_{1/2}$  core. Thus we may expect two series of lines in the electron spectra.

At intensities where 11-photon ionization of Xe by 1064 nm becomes measurable, the electron energies are influenced by the field-gradient force, also called ponderomotive force.<sup>1,7,8</sup> On the one hand, this complicates the analysis of the spectra of multiphoton ionization; on the other hand, the multiphoton ionization gives us the opportunity to study the field-gradient force. In this paper we present a demonstration of the effect of this force.

### II. EXPERIMENTAL

#### A. The laser

A commercial Nd-YAG laser is used (JK system 2000/hyper YAG), giving (10–15)-ns pulses of up to 1 J per pulse at a rate of 10 Hz. The beam is almost single

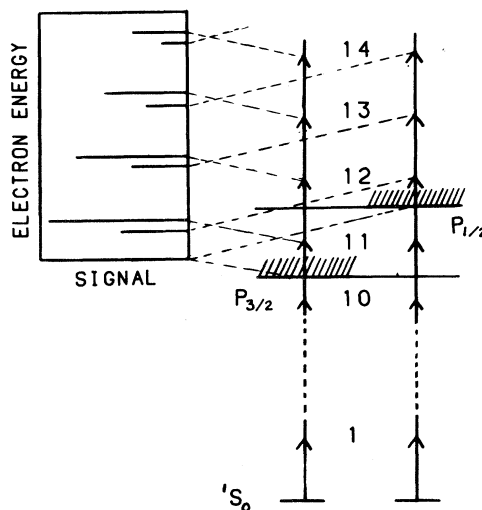


FIG. 1. Energy level diagram of xenon. 11-, 12-, and 13-photon ionization with 1064-nm photons is schematically shown.

mode transversally, but multimode longitudinally; the bandwidth of the 1064-nm light is  $\sim 0.4$  nm, which represents about 400 modes. The light has linear polarization parallel to the direction of detection in the electron spectrometer. For the experiments only the center part of the beam (cross section equal to 2 mm) is selected and focused with a lens of focal length 12 mm. Assuming diffraction-limited focusing, the focus diameter is  $8 \mu\text{m}$ . In the 1064-nm experiments the maximum pulse energy  $F$  at which spectra are taken is  $\sim 35$  mJ, corresponding to an average intensity  $\bar{I}$  in the focus (in  $\text{W}/\text{cm}^2$ ),

$$\bar{I}_{\text{max}} = \frac{F}{\pi/4 d^2 t} = 7 \times 10^{12}. \quad (1)$$

However, due to the chaotic character of the multimode pulse, there will be higher intensities present during short times. The duration of these interference spikes is determined by the bandwidth of the laser. For a bandwidth of 0.4 nm at 1064 nm, a typical duration is 10 ps, while for a number of 400 modes the intensity distribution will look chaotic up to 400 times the average intensity. The intensity distribution for chaotic light is<sup>9</sup>

$$P(I) = \frac{1}{\bar{I}} e^{-I/\bar{I}}. \quad (2)$$

A high-order process is very sensitive to the intensity distribution, because the signal formed at an intensity between  $I$  and  $dI$  is

$$S_N(I)dI = I^N P(I)dI. \quad (3)$$

In chaotic light the ionization takes place around an effective intensity  $I_{\text{eff}}$ , which is higher than the average intensity.  $I_{\text{eff}}$  can be found by calculating at which  $I$  the function  $S_N(I)$  has its maximum. The result is  $I_{\text{eff}} = N\bar{I}$ . The part of the time in which the intensity exceeds  $N\bar{I}$  is  $e^{-N}$ . The effect of the mode structure on multiphoton ionization has been carefully studied.<sup>10</sup> In these earlier studies an effective intensity has been defined as the average intensity of a single-mode pulse yielding the same number of ions as the actual intensity in the experiment. We shall take a slightly different approach and use the definition  $I_{\text{eff}} = N\bar{I}$ , while assuming that the signal arises from picosecond spikes. This way a comparison with single-mode experiments is possible. Also for ponderomotive force effects one has to deal with the effective intensity. A recent study on resonant multiphoton ionization, yielding an experimental distribution function supports the utility of this approach.<sup>11</sup>

From Eq. (1) we find the maximum effective intensity in our experiments for an  $N$ -order process:

$$I_{\text{eff}} = 0.2 \times 10^{12} NF \quad (4)$$

(in  $\text{W}/\text{cm}^2$  if  $F$  is in mJ). It must be stressed here that this is only an estimate of the maximum intensity possible. If the focus is not diffraction limited or the distribution function not quite that of chaotic light, the intensity could be considerably lower.

In some experiments we mixed the fundamental with the second- or third-harmonic beam to get signal from ionization by simultaneous absorption of 1064- and 532-

or 355-nm photons. For such experiments the two beams are focused at the same point by two lenses. The polarization of one of the beams is rotated through  $90^\circ$  to cancel the effect of the doubler crystal. Pulse energies are varied by rotating the polarization direction with a double fresnel rhomb and filtering with a polarizer. In this way we do not influence the intensity distribution in the focus as is known to be the effect of varying the pumping power of the laser rods or inserting neutral density filters. The relative pulse energy is measured in two ways, with an EG & G photodiode and by measuring the angle of rotation of the fresnel rhomb. A calorimeter (Laser Instrumentation) is used for absolute calibration.

### B. The electron spectrometer and signal processing

The electron spectrometer<sup>12</sup> consists of a 50-cm-long flight tube along the axis of which a magnetic field confines the electrons (Fig. 2). The field diverges from a value of 1 T at the laser focus position to  $10^{-3}$  T over a distance of a few millimeters, and then stays constant at this value. The effect of the divergence is the inverse of a magnetic bottle: In the first millimeters of the flight path the electron trajectories are "parallelized" so rigorously that the spread in forward velocities reduces to  $5 \times 10^{-4}$ . The time of flight is then a good measure for the kinetic energy.

Target gas is emitted through a 2-mm hole in one of the pole pieces of the iron circuit that generates the 1-T field. The photoelectrons leave the high-magnitude field region through a 2-mm hole in the second pole piece. The pressure is measured in the flight tube, so we can only estimate the actual pressure in the laser focus by comparing the gas flow through the pole piece with the pumping speed. In this estimation the pressure during our experiments is varied from  $10^{-3}$  to 40 Pa. Background pressure is  $3 \times 10^{-5}$  Pa, which at high intensities still causes problems, especially because of its contribution to the space charge.

In the absence of electrostatic fields at the laser focus, our instrument accepts 50% of all the electrons formed, which has three advantages over standard techniques: (1) the total ion production can be kept low to avoid space-charge effects; (2) the transmission of the instrument is constant down to an electron energy of almost 0 eV; (3) we can easily work out the total ion production and compare this with the number of atoms in the laser focus to make sure that we do not saturate the ionization process.

In order to allow the detection of several hundreds of electrons per laser shot, the signal from the detector is amplified linearly and the total charge as a function of time is recorded on a Philips 3310 (digital) oscilloscope and digitized in 256 time intervals of 20 ns.

In principle we can convert the whole time-of-flight spectrum to an energy spectrum and in this way measure the total range of electron energies at each laser shot. However, the high-energy part of the spectrum will then have a limited resolution because of the finite width of the time channels in the oscilloscope and the pulse duration of the laser. To obtain equal energy resolution for all electron energies only the part of the time-of-flight spectrum from 0.8 to  $1.5 \mu\text{s}$  is converted, corresponding with electron energies from 1.1 to 0.3 eV. The electrons can be ac-

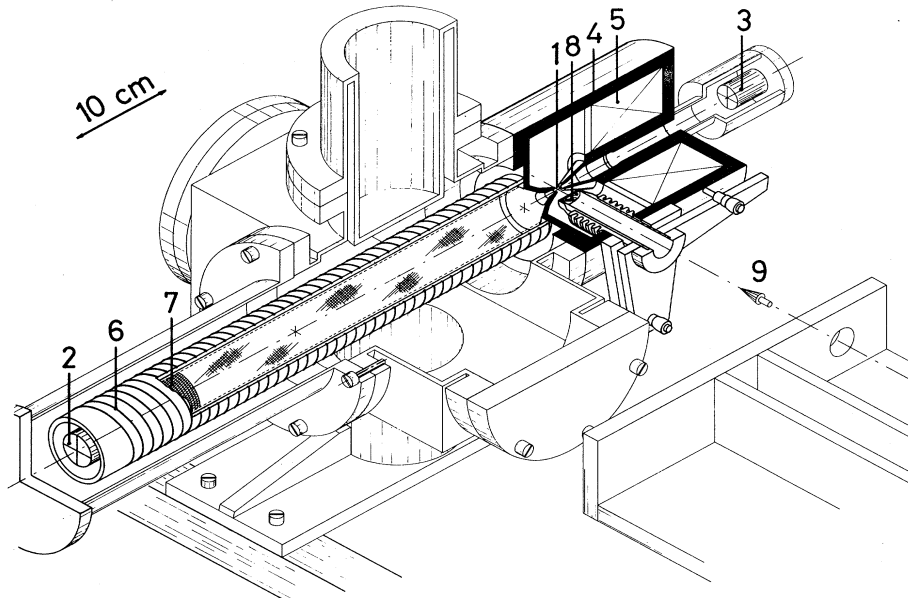


FIG. 2. Electron spectrometer. (1) Laser focus, (2 and 3) electron detectors, (4) iron magnetic circuit giving 1-T field, (5) water-cooled current loops, (6) coil to provide  $10^{-3}$ -T field in the flight tube, (7) grids to change electron velocities, (8) movable lens to focus the laser beam (a similar lens is present at the opposite side), (9) laser beam.

celerated or decelerated just after they have been parallelized in the first part of the flight tube. The deceleration voltage is scanned and taken into account in the time of flight to energy conversion. In this way, giving up some of the efficiency, we obtain a constant resolution of 15 meV.

The detector, consisting of two channel plates in tandem, gives single electron pulses which show a large spread in amplitude. To discriminate the smaller amplitudes against electric noise the average amplitude has to be at least  $\frac{1}{10}$  of the dynamic range of the digitizer. This restricts the maximum number of electrons per time channel to about 10, so in order to observe orders of magnitude differences in ionization probability we have to adjust the pressure in the focus region.

The data from the digitizer are read out into an LSI-11 minicomputer, which sets a software discriminator level and converts the time-of-flight spectrum to an energy spectrum. It also controls the scanning of the decelerating voltage. Resulting spectra are stored in a Digital Equipment Corporation VAX-11/750 computer.

### III. RESULTS AND DISCUSSION

#### A. Relative peak intensities in electron spectra at 1064 nm

Figure 3 shows electron energy spectra arising from ionization of Xe by 1064-nm photons at pulse energies in the range of 10 mJ up to 30 mJ and Xe pressures from 40 Pa down to  $4 \times 10^{-3}$  Pa. The pressures are chosen in such a way that the total electron signal in each spectrum is 25–50 electrons per pulse.

The peak assignment is complicated by the two ionization potentials of Xe. We expect a  $P_{3/2}$  series at  $(0.688 \pm 1.165 \times S)$  eV for  $(11+S)$ -photon ionization and a

$P_{1/2}$  series at  $(0.540 + 1.165 \times S)$  eV for  $(12+S)$ -photon ionization. The energy width of the peaks in Fig. 3 is too great to separate the two series. We address the cause of this width, which is much more than the instrumental resolution, in the section on field gradient force.

An absolute calibration for the energy axis is obtained by comparison with the spectrum from ionization at 532 nm. In this spectrum the  $P_{3/2}$  series is well separated from the  $P_{1/2}$  series and the energy width is less, as will be shown in Fig. 4 and discussed later.

The spectra of Fig. 3 show a considerable probability for continuum-continuum transitions following multiphoton ionization. At the highest intensities measured, the different-order processes even become of the same magnitude.

The most surprising feature in the spectra is the fact that the peak at 0.6 eV (11-photon  $P_{3/2}$  plus 12-photon  $P_{1/2}$ ) grows much more slowly with increasing power than the higher peaks. We have the following arguments to support our claim that this is not an instrumental effect: (i) the peak is well developed at the lowest intensities (that is the highest pressures) that we could measure; (ii) the transmission curve of the spectrometer is flat, as many other experiments (see, e.g., Figs. 4 and 5) have shown; (iii) space charge effects are negligible at the total ion production of 50–100 per laser pulse; (iv) scattering of slow electrons cannot be the cause; the slow electrons disappear at low pressures. At the highest pressures we do expect scattering in the high-pressure region of the instrument, which happens to be also the high magnetic field region (see section on spectrometer). The electrons scattered here will still be parallelized and cannot be distinguished from the electrons that are not scattered.

Comparison with earlier published spectra is possible. In the spectrum of Fabre *et al.*<sup>3</sup> there is at low electron energies only a bump, smaller than the peak at 1.8 eV but

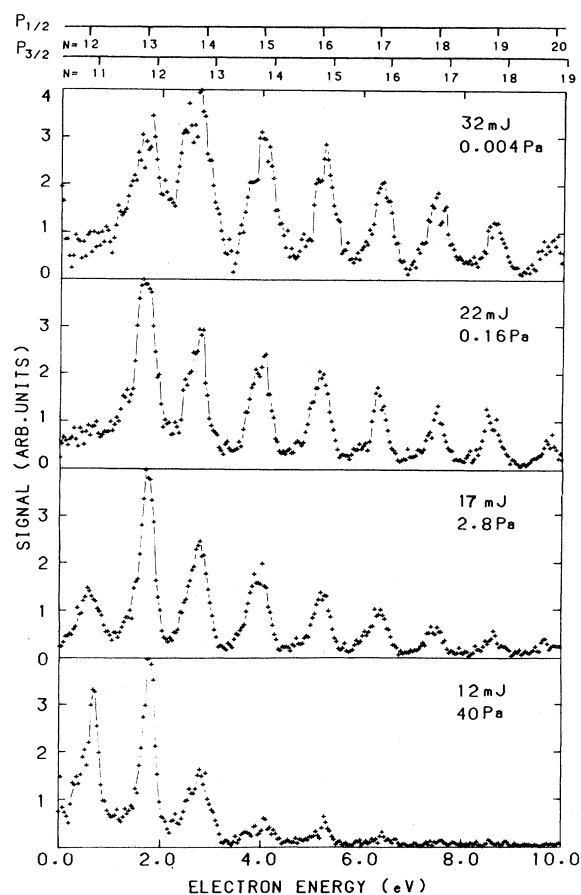


FIG. 3. Electron spectra from multiphoton ionization of xenon at 1064-nm. The vertical scales are normalized. The pulse energy  $F$  and pressure at which each spectrum is taken is given in the figure. In the spectrum at 0.004 Pa, the background has been subtracted. The estimated intensity is  $F(\text{mJ}) \times 2.10^{12} \text{ W/cm}^2$ .

not separated from it. In the preliminary spectrum of Kruit *et al.*<sup>2</sup> the energy axis was determined by self-calibration on the peaks in the spectrum, with the effect that the absence of the first peak gave an erroneous calibration.

It is hard to find an explanation for the apparent suppression of the slow electron peak. From perturbation theory one does expect that at increasing intensity the higher-order peaks will increase as compared to the lower-order peaks. Extrapolating this theory into an intensity regime where it is probably inaccurate, one might predict  $(N+S)$  peaks with higher amplitudes than  $N$  peaks. However, the theoretical description gets complicated here, because higher-order terms give considerable contributions to the  $N$ -photon peak as well. It seems impossible that a straightforward perturbation theory can describe a situation in which the  $N$ -photon peak is absent, while the  $(N+1)$  peak is still the highest in the spectrum.

We suggest that there is a connection between this phenomenon and the fact that 11 photons of 1064 nm are in resonance or near resonance with an autoionizing level. The autoionizing states have a long lifetime compared to pure continuum states. This lifetime could enhance tran-

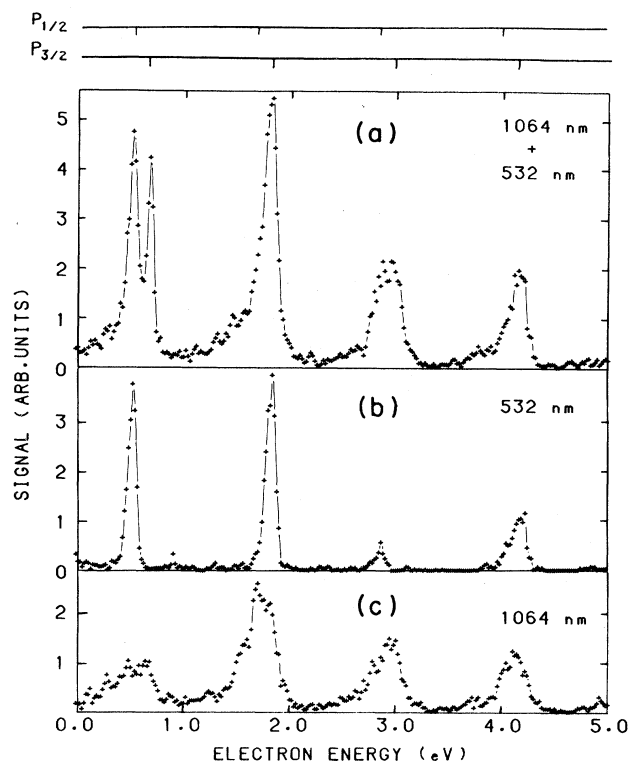


FIG. 4. Electron spectra from ionization of Xe at (a) 1064 and 532 nm, (b) 532 nm, (c) 1064 nm when the beams are focused at the same spot. The spectra from pure 1064 or 532 nm are taken at exactly the same conditions as the spectrum from 1064+532 nm, but with the 532 beam, respectively, the 1064 beam being stopped.

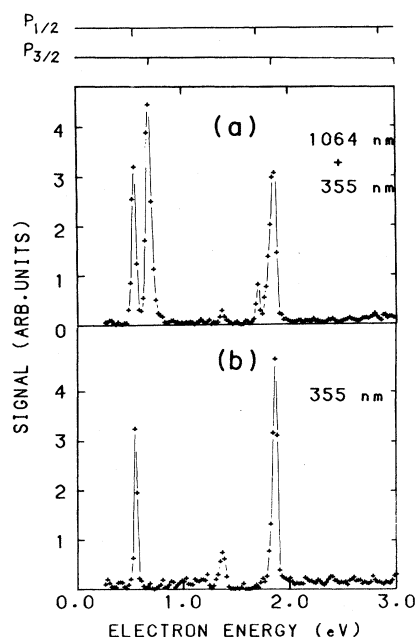


FIG. 5. Electron spectra from ionization of Xe at (a) 355 and 1064 nm and (b) 355 nm when the beams are focused at the same spot.

sitions to higher-lying continuum states before the electron can leave the ion in an 11-photon continuum state. From the tables of Moore<sup>13</sup> we found that the  $7d'$  state is resonant with 11 photons. To check whether this specific resonance has a dramatic effect on the probability for additional photon absorption we created two similar situations: one with, and one without the  $7d'$  as an intermediate resonance. When the 1064- and a 532-nm beams are focused on the same spot, we see (Fig. 4) except from the addition of the pure 1064- and 532-nm spectra also a signal from a process in which one atom has adsorbed a combination of 532- and 1064-nm photons. The  $(5 \times 532 + 1 \times 1064\text{-nm})$  process is now the lowest-order process possible. This combination excites the xenon to the same level in the continuum as the  $(11 \times 1064\text{-nm})$  process but with a different parity, so that the  $7d'$  cannot be excited. Figure 4 shows the result: A high probability for the lowest continuum state with the  $P_{3/2}$  core. Figure 5 shows a similar result for the mixture of 355 and 1964 nm. The  $(3 \times 355 + 2 \times 1064\text{-nm})$  process can excite the  $7d'$  level again. From the rough similarity of the spectra of Figs. 4 and 5 we conclude that it is not specifically the  $7d'$  state that is responsible for the disappearance of the slow-electron peak in the 1064-nm spectra. Figures 4 and 5 also give additional evidence that the  $N$ -photon peaks are the highest in the spectrum if the light intensity is small.

Returning to our suggestion that autoionizing levels can be responsible for the relative decrease of the slow-electron peak, we can add that nearby resonances may play a role because they are ac Stark shifted and lifetime broadened.

A serious problem in this suggested explanation is that it cannot account for the absence of the 12-photon  $P_{1/2}$  peak which is at about the same position in the spectrum as the 11-photon  $P_{3/2}$  peak. It could be however, that ionization to the  $P_{1/2}$  core has a relatively low probability, because it demands the nonresonant absorption of one more photon than the ionization to the  $P_{3/2}$  core.

Both Alimov *et al.*<sup>14</sup> and Lompré *et al.*<sup>15</sup> have scanned the wavelength of a Nd-glass laser in a region close to 1064 nm and measured orders of nonlinearity and total ion yield. Neither of these groups mentions the possibility of autoionizing resonances. It may be doubted whether they are observable in a wavelength scan at such high intensities, because of the lifetime broadening by the transition to the higher-lying continuum.

### B. Orders of nonlinearity

From the series of spectra in Fig. 3 it can be seen that at higher pulse energies, the faster-electron peaks get relatively higher amplitudes. In Fig. 6 the signal in the 1.8-eV peak, the 8.8-eV peak and the total signal are plotted in log-log coordinates as a function of pulse energy. The signal axis, however, is converted to ionization probability by dividing the number of detected electrons by the number

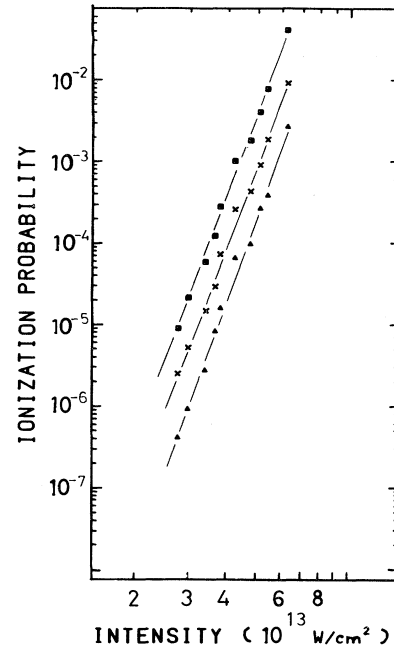


FIG. 6. Ionization probability for  $(N+S)$ -photon ionization of xenon at 1064 nm.  $\square$  total number of electrons;  $\times$  number of electrons in the 1.8-eV peak;  $\triangle$  number of electrons in the 8.7-eV peak as a function of pulse energy. The data come from a series of measurements of which Fig. 3 gives a few examples. The conversion from number of electrons to ionization probability and from pulse energy to intensity is explained in the text.

of atoms in the laser focus. The pulse energy axis is converted to effective intensity as described in Sec. II A. The absolute numbers given in the figure cannot be more than rough estimates.

In Table I the results for the order of nonlinearity  $K$  of a least-squares fit on the data points is shown. The absolute number of the orders of nonlinearity cannot be very accurate. It depends on the linearity of the pressure gauge, the pulse energy measurement and the assumption that our method of varying the pulse energy does not change the intensity distribution function. But the general feature is clear: The orders of nonlinearity for all peaks, except for the slowest, are high and almost equal.

In the data of Fig. 6 no effect is seen of possible saturation. This is consistent with our calculation of total ionization probability. The number of ions that is formed in one laser shot is less than 100. In the focus volume of  $10 \times 10 \times 30 \mu\text{m}^3$ ,  $7.5 \times 10^5 P(\text{Pa})$  atoms are present ( $P$  is the pressure in Pa). This leads to an estimate of about  $10^7$  atoms at the highest pressures and about  $10^3$  at the lowest pressures.

Our results can be compared with a result of Fabre

TABLE I. Order of nonlinearity  $K$  of the peak areas in the spectra of Fig. 3 (least-squares fit).

Peak energy (eV)	0.6	1.8	2.8	4.0	5.2	6.4	7.6	8.7	9.8	Total signal
$K$	7.7	10.0	10.2	10.4	10.8	10.5	10.6	10.5	10.8	10.0

*et al.*<sup>3</sup> These authors measured the order of nonlinearity of the first three peaks in their 1064-nm spectrum and found order 3.4 for all three, from which they concluded that the ionization was saturated. This was at estimated average intensity of a few times  $10^{12}$  W/cm<sup>2</sup>. But comparison is not easy because they used a single-mode pulse. The same authors also reported a study on the order of nonlinearity of the separate electron peaks at 532 nm. In this case saturation could be avoided by keeping the signal low. It is not clear why this could not be done in the 1064-nm study. Lompré *et al.*<sup>15</sup> have performed measurements of the order of nonlinearity for the total ion signal with 30-ps pulses in the intensity regime up to  $1.5 \times 10^{13}$  W/cm<sup>2</sup> and found  $11.0 \pm 0.2$ . We have now demonstrated that at these intensities higher-order processes already play a significant, if not dominant, role. Surprisingly enough our measurements are not in contradiction with those of Lompré *et al.*

Until this moment it has been assumed that perturbation theory gives a good description of multiphoton ionization processes.<sup>3,15,16</sup> Most experimental results could even be described by lowest-order perturbation theory. In this approximation the probability of a process in which  $N+S$  photons are adsorbed increases with the  $(N+S)$  order of the light intensity. If  $(N+S)$ -photon processes have an amplitude comparable with the  $N$ -photon process, higher-order perturbation should be applied also for  $N$ -photon transitions. See, for example, Aymar and Crance,<sup>6</sup> who calculated cross sections for  $(N+S)$ -photon ionization of Cs. Then the rate  $R$  for  $(N+S)$ -photon ionization depends on the intensity as

$$R_{N+S} = \sum_{P=S}^{\infty} a_P I^{N+P}. \quad (5)$$

The coefficient  $a_P$  can be negative for  $P \geq S+1$ . Although it is possible to construct any dependence of  $R$  on  $I$  with this power series, the perturbation theory seems not to be very useful in describing effects that deviate so strongly from lowest order.

The special feature in our data is that all orders of nonlinearity are within the range  $10 \pm 1$ . This seems to indicate that absorption of the first eleven photons acts as a rate-limiting step, followed by continuum-continuum (C-C) transitions which connect the various continua with probabilities close to unity. We have started a calculation of C-C matrix elements for Xe using a model potential. It turns out that for all allowed angular momentum states the calculated C-C transition rates at our highest intensity lead to probabilities on the order of 0.5 or higher. These calculations will be reported in detail elsewhere (Muller and Tip).<sup>17</sup>

In Fig. 7 we plotted the average electron energy in our measurements as a function of effective intensity. It shows a linear dependence:  $\bar{E}_{el} = 0.7 \times 10^{-13} I_{\text{eff}}$  eV. At high intensities the points deviate from the straight line. This is caused by the fact that our measurements stop at an energy of 10 eV. If the trend in the spectra is extrapolated to higher energies, we get estimates for the average energy that do fit the straight line.

As regards this linear relationship, we want to draw attention to the fact that the second stage of the process could also have followed the ionization of the atom by one hard photon or even a process like  $\alpha$  decay.<sup>18</sup> In the

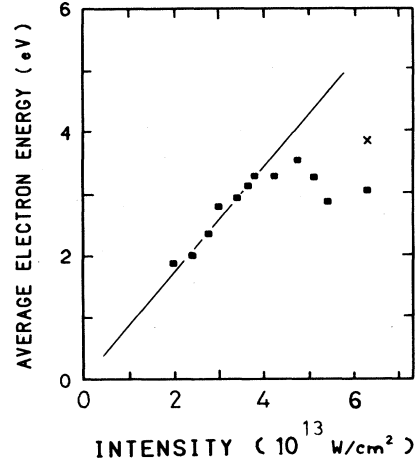


FIG. 7. Average energy of electrons arising from multiphoton ionization of Xe at 1064 nm as a function of intensity. □ data from measurements as in Fig. 3. × background subtracted. Note that the deviation from the straight line at high intensities is a result of the limited energy range (maximum 10 eV) in which the spectra of Fig. 3 are measured.

theory of free-free scattering of electrons<sup>19</sup> the same result has been obtained for the soft-photon limit ( $\hbar\omega \ll E_{el}$ ): The energy gained in the scattering events, averaged over both absorption and emission, is proportional to the light intensity.

### C. Field-gradient force

In the multiphoton experiments on Xe performed with different wavelengths, we find different widths of the peaks in the energy spectra. In Table II we present the minimum width we ever measured. These differences are not the effect of different experimental conditions or different space-charge effects. This is most clearly demonstrated by Fig. 4, which shows a spectrum resulting from ionization by pure 1064-nm light and the effect of adding a 532-nm beam. The additional signal must come from the same point in the spectrometer because it needs both 532- and 1064-nm photons in the same process. Yet the additional signal shows narrower electron peaks.

An explanation can be found in the field-gradient force, also called ponderomotive force. Kibble<sup>7</sup> showed that a free electron can be accelerated by the gradient of an electromagnetic field:

TABLE II. Minimum widths of the peaks in the energy spectra.

$\lambda$ (nm)	$\Delta E_{el}$ (meV)
440 (resonant)	15
355	40
532	60
1064	160

$$F = \frac{-e^2}{4m\omega^2} \nabla |E|^2. \quad (6)$$

This formula shows that a field-gradient effect will be stronger for light with longer wavelength.

Note that electrons in the narrow peaks of Fig. 4(c) are not formed in the high intensity of the 1064-nm light although they come from the same focal area. The pure 1064-nm signal is formed in the high intensity, picosecond duration interference spikes of the 1064-nm beam. The other signal is formed in the high-intensity spikes of the 532-nm beam.

Equation (6) can be integrated over the electron path to find the energy gain of an electron that leaves the focal region<sup>20</sup>:

$$\Delta E = 10^{-13} I \quad (7)$$

(in eV if  $I$  is in  $\text{W}/\text{cm}^2$ ). Note that this quantity  $\Delta E$  is of nearly the same magnitude as the measured average energy. However, the field-gradient force is not expected to increase the average energy, but to cause a shift plus some additional broadening of each of the peaks in the energy spectrum, because not all electrons are formed at the same intensity. In our case the shift would be in the order of 2–7 eV. Absolutely no such shift is observed; we see only a broadening of the order of 200 meV. This cannot be the average over a range of shifts.

A possible explanation could be that the intensity in our focus fluctuates so rapidly that, before the electron is able to escape from the focal region, the intensity has already dropped to the average value. This is not in contradiction to the conservative nature of the gradient force, since we are dealing with a time-dependent field. Remember that because of the multimode character of our pulse the ionization takes place at intensities far above average. Then the electrons are accelerated only part of the way out, with a correspondingly smaller energy gain (see also Ref. 20). Since an electron of 1 eV needs 10 ps to traverse the radius of our focus, the coherence time of the light would have to be less than this, corresponding to a bandwidth of more than 0.1 nm, which is indeed the case in our experiment: We have no etalon in the Nd-YAG laser, resulting in a bandwidth in the order of 0.4 nm. Yet this explanation is unlikely in view of the experiment reported by Fabre *et al.*,<sup>3</sup> in which the predicted peak shift is not observed either, despite the use of single-mode laser pulses of 10-ns duration.

Hollis<sup>8</sup> and Boreham and co-workers<sup>20,21</sup> studied the

electron spectra arising from multiphoton ionization of argon at intensities up to  $10^{15} \text{ W}/\text{cm}^2$  with a low energy resolution. The high electron energies, up to a few hundred eV, were interpreted as being the effect of the field-gradient force. On the basis of our studies it should be reconsidered whether additional photon absorptions have not played a dominant role in the acceleration.

#### IV. CONCLUSIONS

From electron spectra of xenon, ionized at 1064 nm, it was shown that above-threshold ionization can give a considerable contribution to the total ionization signal, at intensities far below saturation. Nevertheless, the order of nonlinearity of the total ionization signal is measured to be close to 11. We interpreted this in terms of an 11-photon rate-limiting step, followed by continuum-continuum transitions with probability near unity.

The electron energy, averaged over the entire spectrum is shown to be proportional to the light intensity. In the electron spectra, the peak corresponding to 11-photon ionization appears relatively suppressed at the high end of our intensity range. The influence of autoionizing levels, increasing the lifetime of the 11-photon state, could account for this.

It was shown that the width of the peaks in the energy spectra is considerably more than the instrumental or space-charge broadening. Field-gradient force is the only reasonable cause, although the energy shift which one would then expect is not observed. The width is only a fraction of the value that theory predicts at our estimated intensities. An explanation for the discrepancy is suggested, but further study, specifically directed towards this subject, is necessary.

*Note added in proof.* A new explanation of the suppression of the low-energy peaks at high intensity has been formulated by Muller and Tip.<sup>17</sup> In a nonperturbative approach, they show that an ac Stark shift of the continuum limit occurs, which for electrons that do escape is exactly canceled by the ponderomotive energy gain.

#### ACKNOWLEDGMENTS

This work was subsidized by the Fundamental Onderzoek der Materie (FOM) and Nederlandse Organisatie voor Zuiver Wetenschappelijk Onderzoek (ZWO).

<sup>1</sup>P. Agostini, F. Fabre, G. Mainfray, G. Petite, and N. K. Rahman, *Phys. Rev. Lett.* **42**, 1127 (1979).

<sup>2</sup>P. Kruit, J. Kimman, and M. J. van der Wiel, *J. Phys. B* **14**, L597 (1981).

<sup>3</sup>F. Fabre, G. Petite, P. Agostini, and M. Clement, *J. Phys. B* **15**, 1353 (1982).

<sup>4</sup>H. B. Bebb and A. Gold, *Phys. Rev.* **143**, 1 (1966).

<sup>5</sup>Y. Gontier, M. Poirier, and M. Trahin, *J. Phys. B* **13**, 1381 (1980).

<sup>6</sup>M. Aymar and M. Crance, *J. Phys. B* **14**, 3585 (1981).

<sup>7</sup>T. W. B. Kibble, *Phys. Rev.* **150**, 1060 (1966).

<sup>8</sup>M. J. Hollis, *Op. Commun.* **25**, 395 (1978).

<sup>9</sup>R. Loudon, *The Quantum Theory of Light* (Clarendon, Oxford, 1972).

<sup>10</sup>C. Lecomte, G. Mainfray, C. Manus, and F. Sanches, *Phys. Rev. A* **11**, 1009 (1975).

<sup>11</sup>P. Kruit, J. Kimman, H. G. Muller, and M. J. van der Wiel, *J. Phys. B* **16**, 937 (1983).

<sup>12</sup>P. Kruit and F. H. Read, *J. Phys. E* **16**, 313 (1983).

<sup>13</sup>C. E. Moore, National Bureau of Standards Circular No. 467 (U.S. GPO, Washington, D.C., 1958).

<sup>14</sup>D. T. Alimov, N. K. Berezhetskaya, G. A. Delone, and N. B.

- Delone, Zh. Eksp. Teor. Fiz. 64, 1178 (1973) [Sov. Phys.—JETP 37, 599 (1974)].
- <sup>15</sup>L. A. Lompré, G. Mainfray, C. Manus, and J. Thebault, Phys. Rev. A 15, 1604 (1977).
- <sup>16</sup>G. Mainfray, in *Proceedings of the Tenth International Conference on the Physics of Electronic and Atomic Collisions*, edited by G. Watel (North-Holland, Amsterdam, 1977), p. 699.
- <sup>17</sup>H. G. Muller and A. Tip (unpublished).
- <sup>18</sup>A. M. Dykhne and G. L. Yudin, Usp. Fiz. Nauk. 121, 157 (1977) [Sov. Phys.—Usp. 20, 80 (1977)].
- <sup>19</sup>C. Jung, Phys. Rev. A 21, 408 (1980).
- <sup>20</sup>B. W. Boreham and B. Luther-Davies, J. Appl. Phys. 50, 2533 (1979).
- <sup>21</sup>K. G. H. Baldwin and B. W. Boreham, J. Appl. Phys. 52, 2627 (1981).